AGU PUBLICATIONS

Geophysical Research Letters

RESEARCH LETTER
10.1002/2014GL061696

Key Points:
- Six year northern Borneo dripwater isotope time series dominated by ENSO variability
- Mixing of vadose waters governs rainfall-to-dripwater isotope transformation
- Different flow pathways produce different dripwater time series from same input

Supporting Information:
- Readme
- Figures S1–S7
- Table S1

Correspondence to:
J. W. Moerman,
jessica.moerman@gatech.edu

Citation:
Moerman, J. W., K. M. Cobb, J. W. Partin, A. N. Meckler, S. A. Carolin, J. F. Adkins, S. Lejau, J. Malang, B. Clark, and A. A. Tuen (2014), Transformation of ENSO-related rainwater to dripwater δ^{18}O variability by vadose water mixing, *Geophys. Res. Lett.*, *41*, doi:10.1002/2014GL061696.

Received 27 AUG 2014
Accepted 24 OCT 2014
Accepted article online 29 OCT 2014

Transformation of ENSO-related rainwater to dripwater δ^{18}O variability by vadose water mixing

Jessica W. Moerman[1], Kim M. Cobb[1], Judson W. Partin[2], A. Nele Meckler[3], Stacy A. Carolin[4], Jess F. Adkins[5], Syria Lejau[6], Jenny Malang[6], Brian Clark[6], and Andrew A. Tuen[7]

[1]School of Earth and Atmospheric Sciences, Georgia Institute of Technology, Atlanta, Georgia, USA, [2]Institute for Geophysics, Jackson School of Geosciences, University of Texas at Austin, Austin, Texas, USA, [3]Geological Institute, ETH Zürich, Zürich, Switzerland, [4]Department of Earth Sciences, University of Oxford, Oxford, UK, [5]Division of Geological and Planetary Sciences, California Institute of Technology, Pasadena, California, USA, [6]GunungMulu National Park, Sarawak, Malaysia, [7]Institute of Biodiversity and Environmental Conservation, Universiti Malaysia Sarawak, Sarawak, Malaysia

Abstract Speleothem oxygen isotopes (δ^{18}O) are often used to reconstruct past rainfall δ^{18}O variability, and thereby hydroclimate changes, in many regions of the world. However, poor constraints on the karst hydrological processes that transform rainfall signals into cave dripwater add significant uncertainty to interpretations of speleothem-based reconstructions. Here we present several 6.5 year, biweekly dripwater δ^{18}O time series from northern Borneo and compare them to local rainfall δ^{18}O variability. We demonstrate that vadose water mixing is the primary rainfall-to-dripwater transformation process at our site, where dripwater δ^{18}O reflects amount-weighted rainfall δ^{18}O integrated over the previous 3–10 months. We document large interannual dripwater δ^{18}O variability related to the El Niño–Southern Oscillation (ENSO), with amplitudes inversely correlated to dripwater residence times. According to a simple stalagmite forward model, asymmetrical ENSO extremes produce significant offsets in stalagmite δ^{18}O time series given different dripwater residence times. Our study highlights the utility of generating multiyear, paired time series of rainfall and dripwater δ^{18}O to aid interpretations of stalagmite δ^{18}O reconstructions.

1. Introduction

The broad geographic availability of speleothems has allowed for the generation of continuous high-resolution, absolutely dated paleoclimate reconstructions from oxygen isotopes (δ^{18}O) across the globe. As a key tropical link between high-latitude, high-resolution ice core and tropical, low-resolution marine sediment records, speleothems have served to constrain the global extent of glacial terminations [e.g., *Cheng et al.*, 2009; *Meckler et al.*, 2012], characterize millennial-scale abrupt climate changes [e.g., *Wang et al.*, 2001; *Carolin et al.*, 2013], provide evidence of interhemispheric antiphasing in terrestrial hydroclimate [e.g., *Cruz et al.*, 2005a; *Wang et al.*, 2006; *Griffiths et al.*, 2009; *Ayliffe et al.*, 2013], and reconstruct centennial-scale variability over the last millennium [e.g., *Sinha et al.*, 2007; *Zhang et al.*, 2008; *Partin et al.*, 2013b]. Annually and subannually resolved speleothem δ^{18}O records also track high-frequency tropical modes, such as the El Niño–Southern Oscillation (ENSO) [e.g., *Lachniet*, 2004], monsoon variability [e.g., *Fleitmann et al.*, 2004; *Berkelhammer et al.*, 2010], and tropical cyclones [e.g., *Frappier et al.*, 2007].

The amount effect—whereby rainfall δ^{18}O in lower latitudes is inversely correlated to rainfall amount [*Dansgaard*, 1964; *Rozanski et al.*, 1993]—forms the basis for interpretations of low-latitude speleothem δ^{18}O as records of past hydroclimate variability. More recently, attention has turned toward site-specific investigations of the isotope-climate relationship through time, using long-term observational monitoring programs [e.g., *Cobb et al.*, 2007; *Kurita et al.*, 2009; *Vimeux et al.*, 2011; *Moerman et al.*, 2013] and isotope-equipped general circulation models (GCMs) [e.g., *Schmidt et al.*, 2007; *LeGrande and Schmidt*, 2009; *Lewis et al.*, 2010]. While broadly supporting the amount effect relationship in the tropics, these studies and others [e.g., *Lawrence et al.*, 2004] suggest that δ^{18}O variability is best interpreted as a reflection of regional-scale, rather than local, hydrological variability. GCM and observation-based studies by *Schmidt et al.* [2007] and *Moerman et al.* [2013], respectively, further document that local rainfall δ^{18}O outperforms local precipitation amount as an indicator of large-scale atmospheric circulation. Such studies lend strong support to the use of speleothem-based reconstructions of rainfall δ^{18}O for tracking low-frequency modes of hydroclimate variability.

Surface-to-cave infiltration modifies the original rainfall $\delta^{18}O$ signal, yet this transformation is poorly constrained for all but a few karst systems. *Baker et al.* [2012] suggest that karst hydrology may even be a stronger control on speleothem $\delta^{18}O$ variability than climate, in extreme cases, highlighting the need for additional studies on this topic. Dominant transformation processes include evaporation of water within the soil and epikarst layers [e.g., *Ayalon et al.*, 1998; *Bradley et al.*, 2010], biases in hydrologically effective recharge toward high-volume rainfall events and/or wet seasons [e.g., *Jex et al.*, 2010; *Pape et al.*, 2010; *Partin et al.*, 2012], mixing in the vadose zone [e.g., *Partin et al.*, 2012; *Genty et al.*, 2014], and variable water routing [e.g., *Baker et al.*, 2012; *Jex et al.*, 2013; *Treble et al.*, 2013]. Nonstationary and nonlinear flow behavior may further obscure the relationship between rainfall and dripwater $\delta^{18}O$ [*Bradley et al.*, 2010; *Baker et al.*, 2013]. As no two cave systems are alike, temporal monitoring of dripwater $\delta^{18}O$ at individual paleoclimate sites is essential to constrain the unique influence of karst hydrology on speleothem $\delta^{18}O$ and improve interpretations of past climate variations.

Here we present a new 6.5 year, biweekly collected time series of dripwater $\delta^{18}O$ from the Mulu karst system in northern Borneo, where tropical hydroclimate has been reconstructed over the past 500,000 years [*Partin et al.*, 2007; *Meckler et al.*, 2012; *Carolin et al.*, 2013]. Building upon previous work by *Cobb et al.* [2007] and *Partin et al.* [2013a], this paper seeks to characterize Mulu karst hydrology and its impact on the dripwater $\delta^{18}O$ variability that is ultimately archived in Borneo speleothem $\delta^{18}O$. By comparing Mulu rainfall and dripwater $\delta^{18}O$ time series, we identify the dominant karst transformation processes at Mulu, estimate water transit times, and demonstrate how different residence times can influence speleothem $\delta^{18}O$.

2. Geological and Climatic Setting

The caves of Gunung Mulu National Park are found in northwestern Borneo (4°N, 114°E) within the Melinau Limestone Formation—a late Eocene to early Miocene shallow marine carbonate platform [*Wilford*, 1961; *Wannier*, 2009]. The site receives approximately 5 m of precipitation annually, which supports lush tropical rainforests with relatively thin topsoil. Seasonality in both precipitation amount and rainfall $\delta^{18}O$ is weak due to the site's year-round position within the Intertropical Convergence Zone [*Cobb et al.*, 2007; *Moerman et al.*, 2013]. The largest anomalies in precipitation amount and rainfall $\delta^{18}O$ occur intraseasonally in association with the Madden-Julian Oscillation (MJO; 30–90 days) and interannually in association with ENSO (2–7 years), with La Niña (El Niño) events delivering anomalously wet (dry) conditions to the region [*Moerman et al.*, 2013]. Recharge for the Mulu karst system can be broadly divided into three categories: (1) autogenic infiltration of precipitation falling directly onto the Melinau limestone; (2) allogenic runoff from the adjoining sandstone mountain Gunung Mulu (2377 m); and (3) occasional flooding of the Melinau River alluvial plain [*Waltham and Brook*, 1980].

3. Methods

Two distinct dripwater sampling programs were launched for this study: (1) a biweekly collection of dripwater at three individual drip sites from May 2006 to November 2012 and (2) spatial surveys of stalagmite-forming drips throughout multiple caves and chambers during three field expeditions in August 2008 ($N = 36$), February–March 2010 ($N = 54$), and October–November 2012 ($N = 135$).

For the 6.5 year dripwater time series, discrete samples were collected by park staff approximately every 2 weeks. Drip rate was measured manually via stopwatch. Two of the dripwater time series were collected from Wind Cave and the third from Lang's Cave, approximately 5 km to the south [*Partin et al.*, 2013a]. The two Wind Cave drips are located 50–75 m from the entrance and overlain by ~100 m of bedrock. The first drip site, named Wind Slow (WS), has a relatively slow drip rate of 7 ± 1 dpm (drips per minute; 1σ) and drips onto bedrock detritus (Figure S1 in the supporting information). The second site, named Wind Fast (WF), has a relatively fast drip rate of 35 ± 6 dpm (1σ) and drips into a small pool within a speleothem (Figure S1). The Lang's Cave drip site (L2) is located approximately 140 m from the entrance and overlain by ~200 m of bedrock. L2 has an average drip rate of 14 ± 3 dpm (1σ) and drips onto a 2 m tall stalagmite (Figure S1).

This study also extends the Mulu rainfall $\delta^{18}O$ time series presented in *Moerman et al.* [2013] by 1.5 years. All rainfall and dripwater samples were collected in 3 mL glass vials and sealed with rubber stoppers and crimp top aluminum closures to safeguard against postcollection evaporation. Rainfall and dripwater $\delta^{18}O$ and δD were analyzed via cavity ring-down spectroscopy (Picarro L1102-i water isotope analyzer), which has a long-term reproducibility of ±0.1‰ for $\delta^{18}O$ and ±0.8‰ for δD (1σ) [*Moerman et al.*, 2013].

4. Results

4.1. Observed Mulu Dripwater $\delta^{18}O$ Variability

The oxygen isotopic composition of the three dripwater time series varies coherently through time despite considerable diversity in drip type, drip rate, and geographic location (Figure 1c). Despite the large difference in drip rate, the Wind Cave drips WF and WS exhibit the same range of $\delta^{18}O$ variability (–4.9 to –11.6‰) and nearly identical mean isotopic values (-8.2 ± 1.2‰ (1σ) and -8.0 ± 1.2‰ (1σ), respectively). Drip L2 in Lang's Cave has a similar mean $\delta^{18}O$ value of -8.4 ± 0.6‰ (1σ), but the amplitude of the variability (-7.2 to -10.0‰) is roughly half that of WF and WS. Variations in drip rate are poorly correlated to dripwater $\delta^{18}O$ variability (Figures 1c and 1d; $R < 0.1$).

The isotopic maximum for each time series occurs during the moderate 2009/2010 El Niño event, whereas the isotopic minimum coincides with a weak La Niña event in 2008/2009 (Figures 1a and 1c). Rainfall and dripwater $\delta^{18}O$ anomalies related to El Niño events are larger in magnitude, shorter in duration, and decay more rapidly than those associated with La Niña events, reflecting asymmetry in the duration and magnitude of El Niño versus La Niña events themselves [e.g., *McPhaden and Zhang*, 2009; *Okumura and Deser*, 2010]. The El Niño-related anomalies in WF and WS are 2–3‰ heavier than those observed in L2. The La Niña-related dripwater $\delta^{18}O$ anomalies are more similar across the drip sites, clustering within 1‰ of each other during moderate-to-strong La Niña events (Figure 1c).

A succession of several intense precipitation events in late 2008/early 2009 associated with a particularly active MJO [*Moerman et al*., 2013] contributes to the minimum in dripwater $\delta^{18}O$ observed during this time. This package of relatively frequent, large precipitation events is unique in the time series, and its relationship to the concurrent La Niña event is unclear, as the other weak La Niña event (2011/2012) covered in the study period is not associated with particularly active MJO activity. Generally speaking, however, intraseasonal rainfall $\delta^{18}O$ anomalies of ~10‰ [*Moerman et al*., 2013] are largely homogenized in the resulting dripwater $\delta^{18}O$ time series, leaving a predominantly interannual signal related to ENSO variability.

The three dripwater $\delta^{18}O$ time series reflect smoothed, lagged versions of amount-weighted Mulu rainfall $\delta^{18}O$ (Figures 1b and 1c). Relative to the 6–8‰ ENSO-related variations in Mulu rainfall $\delta^{18}O$ (Figure 1b) [*Moerman et al*., 2013], interannual variability is reduced to ~5‰ in the Wind Cave drips and to ~2.5‰ in L2. The timing of dripwater $\delta^{18}O$ maxima and minima also lags rainfall $\delta^{18}O$ by 2–3 months. Taken together, this suggests that mixing of infiltrating waters is a dominant influence on the resultant isotopic composition of dripwater at the monitored sites. Potential biases in recharge rates during wet versus dry times, as well as potential evaporative enrichment of soil water, both appear to have limited influence on dripwater $\delta^{18}O$, as evidenced by (i) the close match between mean amount-weighted Mulu rainfall $\delta^{18}O$ (-8.6 ± 3.5‰ (1σ)) and the combined mean isotopic value for the three dripwater time series (-8.2 ± 1.0‰ (1σ); Figure 1c) and (ii) the lack of consistent evaporation tails in plots of dripwater $\delta^{18}O$ versus δD (Figure S2).

4.2. Residence Time Analysis

To further probe karst hydrology as it relates to the rainfall-to-dripwater $\delta^{18}O$ transformation, we model dripwater $\delta^{18}O$ from the daily Mulu rainfall $\delta^{18}O$ time series. We begin by considering a simple recharge model wherein a single reservoir is fed by the autogenic infiltration of percolating precipitation. We simulate the effect of different mixing rates on dripwater $\delta^{18}O$ variability by averaging daily amount-weighted rainfall $\delta^{18}O$ over the previous n weeks (e.g., backward projected running mean). In this way, we generate a suite of modeled dripwater $\delta^{18}O$ time series corresponding to different residence times (Figure S3) and infer the actual residence time to be the number of weeks used in the modeled dripwater time series that best correlates with the observed time series for each drip site (Figure S4).

We estimate residence times of 3–4 months for reservoirs feeding drips WF and WS. Observed dripwater $\delta^{18}O$ variations in WF are best reproduced by averaging amount-weighted rainfall $\delta^{18}O$ over the previous 13 weeks or ~3 months ($R = 0.92$; Figure 2), while WS is best correlated to the modeled time series with an 18 week or ~4 month averaging interval ($R = 0.94$; Figure 2). For these two drips, our simple autogenic recharge model reproduces both the variability and amplitude of variance extremely well and captures the observed lag between rainfall and dripwater $\delta^{18}O$ minima and maxima.

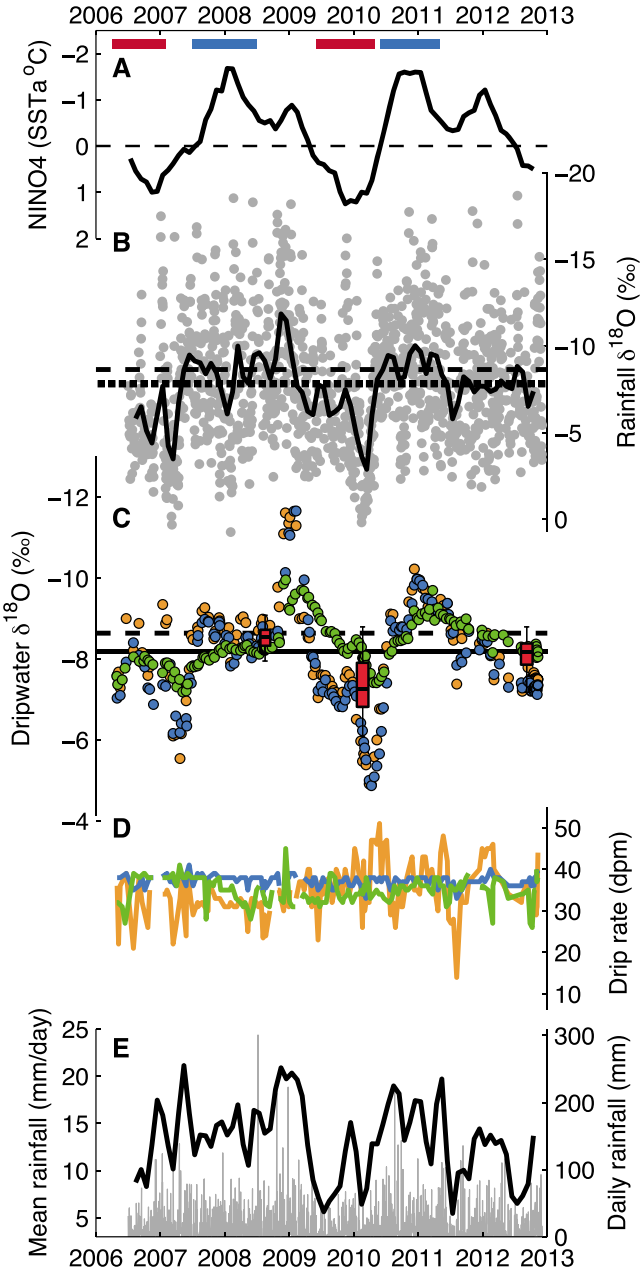

Figure 1. Comparison of Mulu dripwater δ^{18}O to rainfall δ^{18}O and local and regional climate variables. (a) Monthly NINO4 SST anomalies [*Reynolds et al.*, 2002]. Red and blue bars along the upper *x* axis represent weak-to-moderate El Niño and moderate-to-strong La Niña events as defined by the Oceanic Niño Index (http://www.cpc.ncep.noaa.gov/products/analysis_monitoring/ensostuff/ensoyears.shtml). (b) Nonamount-weighted daily Mulu rainfall δ^{18}O (gray circles) shown with a 2 month running average (black line), and nonamount-weighted (dotted line) and amount-weighted (dashed line) means of the entire time series. (c) Mulu dripwater δ^{18}O from drips WF (orange), WS (blue), and L2 (green) plotted with the composite mean of the three dripwater δ^{18}O time series (black line) and mean amount-weighted rainfall δ^{18}O from Figure 1b (dashed line). Box-and-whisker plots represent the median (bold bar), 25–75% quartile range (red box), and maximum and minimum δ^{18}O values (whiskers) for system-wide field expedition surveys of stalagmite-forming dripwaters conducted in August 2008 ($n = 36$), February–March 2010 ($n = 54$), and October–November 2012 ($n = 135$). (d) Drip rates from drip sites WF (orange), WS (blue), and L2 (green). Note that WS drip rate has been shifted by +30 dpm and L2 by +20 dpm. (e) Rain gauge measurements of daily Mulu precipitation amount (gray bars) plotted with a 2 month running average (black line). *Y* axes in Figures 1a–1c are inverted.

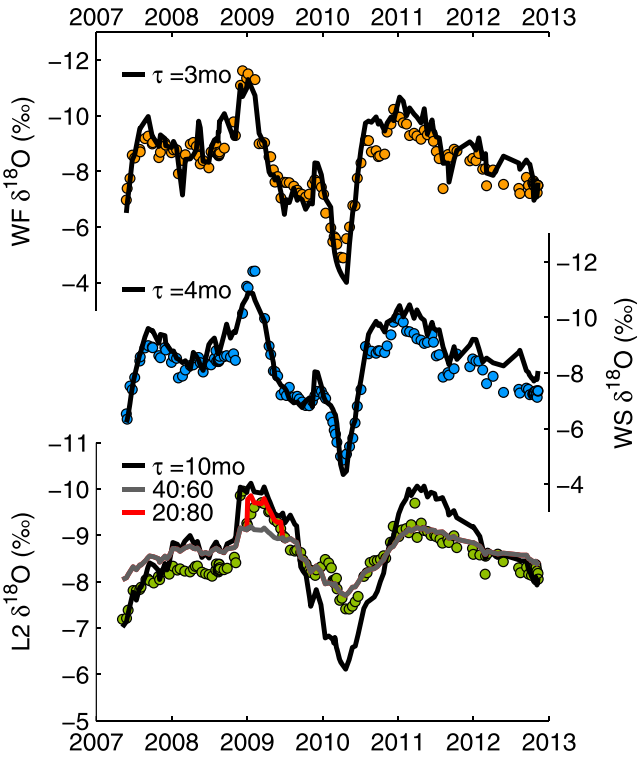

Figure 2. Observed dripwater δ^{18}O (circles) for drips WF (orange), WS (blue), and L2 (green) compared with best fit modeled dripwater δ^{18}O (solid lines) using amount-weighted Mulu rainfall δ^{18}O as input. Bold black lines represent dripwater simulated by the autogenic recharge model with a residence time of ~3 months for WF, ~4 months for WS, and ~10 months for L2. Bivariate mixing model results for drip L2 modeled as 40% of Reservoir A with an ~10 month residence time and 60% of Reservoir B reflecting mean amount-weighted rainfall δ^{18}O are plotted as a gray line. During the October 2008 to June 2009 interval, the red line reflects modeled dripwater δ^{18}O assuming contributions of 20% from Reservoir A and 80% from Reservoir B. *Y* axes are inverted in all panels.

While the autogenic recharge model reproduces the timing of L2 dripwater δ^{18}O minima and maxima, it overestimates the amplitude of the drip's δ^{18}O variations (Figure 2). Amount-weighted rainfall δ^{18}O averaged over the previous 42 weeks (~10 months) best reflects the timing of dripwater δ^{18}O maxima and minima observed in L2 ($R = 0.84$), but the predicted variations are roughly 1‰ higher than observed (Figure 2). This suggests that the flow pathway to this drip site is more complicated than that feeding WF and WS. L2's amplitude attenuation suggests a likely contribution from a second, well-mixed reservoir, which we model using a bivariate mixing model,

$$\mathbf{X_M} = \mathbf{X_A}(1 - f_B) + \mathbf{X_B} f_B \qquad (1)$$

where $\mathbf{X_A}$ is the isotopic composition of Reservoir A, $\mathbf{X_B}$ is the isotopic composition of Reservoir B, and f_B is the mixing parameter. Modeled dripwater δ^{18}O simulated by the autogenic recharge model with an ~10 month residence time represents Reservoir A. In the interest of simplicity, we set the isotopic composition of Reservoir B as amount-weighted Mulu rainfall δ^{18}O averaged across the study period (−8.6‰). At $f_B = 0.6$, the residuals between the modeled and observed L2 time series are minimized. With this model configuration, the muted variability in L2 is reproduced particularly well during the 2009–2012 ENSO cycle (Figure 2), suggesting that two distinct reservoirs likely feed L2—one with a residence time of ~10 months that is recharged autogenically (Reservoir A) and a second with a significantly longer residence time (Reservoir B). However, prior to 2009, the above parameters overdamp the variability, resulting in a poor fit between the modeled and observed time series. Increasing the Reservoir A flux from 40% to 80% (i.e., $f_B = 0.2$) during late 2008/early 2009 greatly improves model-data fit, suggesting an abrupt switch in flow to L2 during this period (Figure 2). Indeed, Reservoir A may represent 100% of flow in December 2008. Throughout 2008, modeled dripwater δ^{18}O is ~0.5‰ more negative than observed L2 values, indicating that either (i) the isotopic composition of Reservoir B varies over the study period and/or (ii) that our simple two-reservoir model fails to capture the complexity of flow feeding L2. Longer time series of rainwater and dripwater δ^{18}O are required to differentiate between these scenarios.

The isotopic spread of hundreds of stalagmite-forming drips collected during field expeditions falls within the variability of the dripwater δ^{18}O time series (Figure 1c), indicating that the three time series drips are broadly representative of system-wide shifts in isotopic composition. The relatively small spread in both the 2008 and 2012 expedition data sets (~0.3‰ (1σ)) suggests that residence times for stalagmite-forming drips in Mulu are long enough to homogenize large intraseasonal shifts in rainfall δ^{18}O of ~10‰ [*Moerman et al.*, 2013], establishing a lower bound for residence times of stalagmite-forming drips of approximately 1–2 months. Likewise, residence times for many stalagmite-forming drips appear to be less than 2 years, as only 25% of the 2010 expedition drip distribution overlaps that of the 2008 expedition (Figure 1c). This remains true even when a subset of the slowest dripping samples (<2 dpm) is considered.

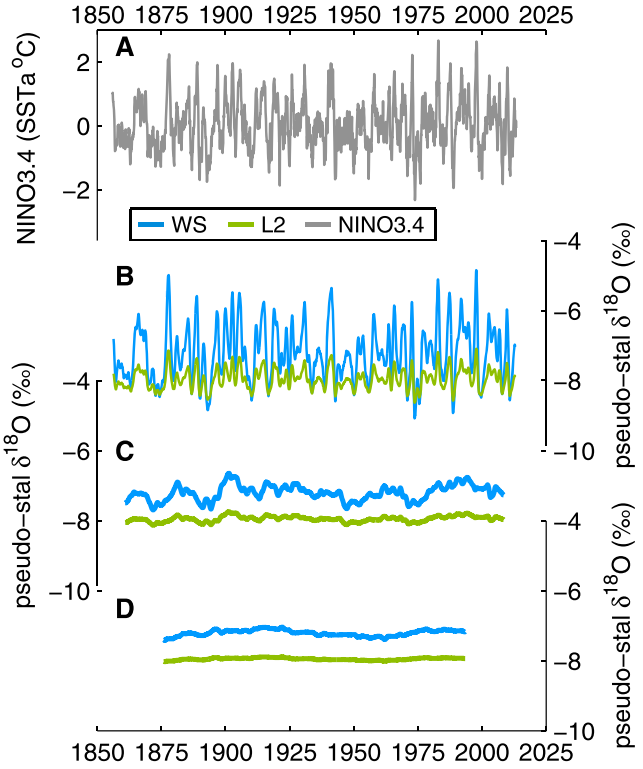

Figure 3. Pseudostalagmite δ^{18}O time series obtained by converting the NINO3.4 SST index into a time series of dripwater δ^{18}O using the observed relationship between NINO3.4 and dripwater δ^{18}O time series during the study interval. (a) Extended NINO3.4 index retrieved from http://iridl.ldeo.columbia.edu/SOURCES/.Indices/.nino/ [*Reynolds et al.*, 2002]. (b) Annually resolved, (c) 10 year resolution, and (d) 40 year resolution pseudostalagmite δ^{18}O modeled from observed WS (blue) and L2 (green) dripwater δ^{18}O.

4.3. ENSO-Related Pseudostalagmite δ^{18}O Variability

To explore how ENSO variability may be recorded in high- and low-resolution stalagmite δ^{18}O reconstructions, we generate pseudostalagmites from the dripwater δ^{18}O time series and sample them at a variety of temporal resolutions. First, we transform the NINO3.4 sea surface temperature (SST) index over the last 150 years into pseudodripwater δ^{18}O space using scalings obtained from drip WS or L2 (WF is similar to WS, for these purposes). Specifically, we perform a peak-to-peak linear regression between observed dripwater δ^{18}O time series and the NINO3.4 SST index over the study period (Figure S5) [*Kaplan et al.*, 1998]. Next, we sample the pseudodripwater δ^{18}O time series at annual to multidecadal resolutions to reflect typical stalagmite growth rates. As our approach assumes that pseudostalagmite δ^{18}O is a perfect recorder of ENSO dripwater δ^{18}O variability, this analysis represents an upper bound on possible ENSO-related stalagmite δ^{18}O variability.

Differences in dripwater residence time lead to large differences between the WS and L2 pseudostalagmite δ^{18}O time series (Figure 3). When sampled at annual resolution, ENSO variability in pseudostalagmite WS is as large as 4‰ versus 1.5‰ for pseudostalagmite L2, as positive El Niño-related δ^{18}O anomalies are damped more effectively in L2 (Figure 3b). At decadal sampling resolution, individual ENSO events are largely unresolvable in the pseudostalagmites (Figure 3c), as expected. However, for decadal sampling, periods of high ENSO variance (e.g., 1970–2000) result in pseudostalagmite δ^{18}O values that are lower than those during ENSO quiescent periods (e.g., 1920–1960). The asymmetrical nature of the ENSO phenomenon, whereby El Niño events produce higher-amplitude anomalies than La Niña events [e.g., *McPhaden and Zhang*, 2009], imparts a shift in mean pseudostalagmite δ^{18}O during high- versus low-variance periods.

At all sampling resolutions, the mean δ^{18}O value for pseudostalagmite L2 is ~0.8‰ heavier than pseudostalagmite WS, similar to mean δ^{18}O offsets of up to ~0.7‰ observed between individual Borneo stalagmite records [*Partin et al.*, 2007; *Carolin et al.*, 2013]. To determine the cause of this offset, we generate pseudostalagmites from modeled dripwater δ^{18}O with different parameterization schemes to isolate the effects of (1) dripwater residence time, (2) multiple reservoirs, and (3) precipitation amount weighting (Figure S6; see the supporting information for details). We find that dripwater residence time accounts for the majority of the observed offset, whereby drips with longer residence times are biased toward lower, La Niña-like δ^{18}O values, given the asymmetry of the ENSO phenomenon. Amount weighting of rainfall δ^{18}O also contributes to the observed offset by driving pseudostalagmite L2 toward even lower δ^{18}O values (Figure S6), as La Niña events are associated with higher precipitation amount at the site. As such, we conclude that the observed offset can be attributed to the combination of different dripwater residence times, ENSO asymmetry, and the latter's impact on amount-weighted rainfall δ^{18}O.

5. Discussion

This study is one of the first to capture individual ENSO events in dripwater $\delta^{18}O$. Previous work by *McDonald* [2004] documented ENSO variability in dripwater trace metal composition, while *Frappier et al*. [2002] found clear evidence of ENSO in a high-resolution stalagmite $\delta^{13}C$ record. The large range of variability exhibited in Mulu dripwater $\delta^{18}O$ (3–7‰) stems from relatively short residence times (3–10 months) compared to the dominant input frequency (i.e., interannual). While similarly large dripwater $\delta^{18}O$ variations are reported elsewhere [e.g., *Ayalon et al*., 1998; *Oster et al*., 2012], these sites typically involve rapid flow through karst conduits and joints, such that dripwater $\delta^{18}O$ time series reflect discrete rainfall events. Flow to the temporally monitored drips at Mulu, however, is likely delivered by diffuse seepage flow [*Cobb et al*., 2007; *Partin et al*., 2013a]. Given the dominance of seasonal variability at most other cave monitoring sites with diffuse flow, large seasonal variations in rainfall $\delta^{18}O$ (>4‰) are largely smoothed out by residence times greater than a year, generating dripwater $\delta^{18}O$ variability of only ~1‰ [e.g., *Mickler et al*., 2004; *Cruz et al*., 2005b; *Pape et al*., 2010; *Partin et al*., 2012; *Treble et al*., 2013; *Genty et al*., 2014].

Given the preservation of resolvable ENSO-related variations in dripwater $\delta^{18}O$, annual and higher-resolution $\delta^{18}O$ records from fast-growing Borneo stalagmites are likely to capture ENSO-related variability. However, our analyses indicate that several factors may influence the variance of interannual stalagmite $\delta^{18}O$ signals. Most significantly, we find that different flow pathways and mixing rates can produce different dripwater $\delta^{18}O$ time series, even given the same rainfall $\delta^{18}O$ input, consistent with karst system modeling studies [e.g., *Bradley et al*., 2010; *Baker et al*., 2012, 2013] and observations elsewhere [e.g., *Ayalon et al*., 1998; *Treble et al*., 2013; *Genty et al*., 2014]. Specifically, longer transit times attenuate dripwater $\delta^{18}O$ variance more effectively and enhance temporal lags between the original rainfall $\delta^{18}O$ (climate) signal and the dripwater $\delta^{18}O$ (speleothem) signal. Therefore, stalagmites fed by water with a relatively short residence time will exhibit higher ENSO-related $\delta^{18}O$ variance than those associated with longer transit times, as demonstrated by our pseudostalagmite model. As such, stalagmite $\delta^{18}O$ is best suited for inferring relative changes in ENSO variance, assuming that dripwater residence time is relatively stable through time. There is evidence that sustained bursts of strong MJO-related convective activity may produce dripwater $\delta^{18}O$ anomalies on the order of those associated with a strong La Niña event (i.e., -2 to -3‰), but such events are rare in the observed time series. The contribution of higher-frequency and lower frequency climate signals to dripwater $\delta^{18}O$ variability awaits the generation of longer rainfall and dripwater $\delta^{18}O$ time series.

Our study provides compelling evidence that some drips are characterized by nonstationary flow regimes, which would complicate the interpretation of climate-related signals in the resulting stalagmite $\delta^{18}O$ records. Potential drivers of nonstationary flow include changes in the nature of rainfall events delivering infiltrating waters, changes in karst water balance, and reservoir volume thresholds that may bias flow along certain pathways [*Bradley et al*., 2010; *Baker et al*., 2013]. Indeed, a change in water routing to drip L2 in late 2008 following unusually wet conditions resulted in more negative dripwater $\delta^{18}O$ values than expected under stationary flow conditions. This abrupt change in flow suggests that some drips at Mulu may be sensitive to karst water balance and/or thresholds in reservoir volume. Additionally, the fact that karst hydrology alters the amplitude and timing of water isotopic extrema in a nonuniform, and potentially nonlinear, manner introduces the possibility that relationships between climate-related fields and stalagmite $\delta^{18}O$ may not always be stationary over time. This is an important consideration for high-resolution studies that rely on modern calibrations between rainfall, dripwater, or stalagmite $\delta^{18}O$ and instrumental climate variables to derive quantitative estimates of past climatic conditions from high-resolution stalagmite $\delta^{18}O$ reconstructions, as emphasized elsewhere [e.g., *Bradley et al*., 2010; *Baker et al*., 2013; *Jex et al*., 2013]. The generation of multiple stalagmite $\delta^{18}O$ records that overlap in time allows for the separation of climatic versus nonclimatic influences on stalagmite $\delta^{18}O$, under the assumption that climate-related $\delta^{18}O$ variations are well-replicated across samples [*Dorale and Liu*, 2009].

At multidecadal and longer timescales, Borneo stalagmite $\delta^{18}O$ likely reflects the long-term mean of amount-weighted rainfall $\delta^{18}O$. Our pseudostalagmite analysis demonstrates that multidecadal changes in ENSO variance on the order of those observed during the instrumental record [*Kleeman and Power*, 2000] can produce lower frequency isotopic variability of similar magnitude to the ~0.5‰ centennial-scale variations observed in low-resolution Borneo stalagmite $\delta^{18}O$ records [*Partin et al*., 2007; *Carolin et al*., 2013]. However,

the rectification of changes in ENSO variance cannot explain the 1–3‰ variations of stalagmite δ^{18}O documented on millennial to orbital timescales [*Partin et al*., 2007; *Meckler et al*., 2012; *Carolin et al*., 2013]. That said, our study confirms the sensitivity of rainfall and dripwater δ^{18}O variations in northern Borneo to zonal shifts in the location of deep convection in the western Pacific [*Moerman et al*., 2013], which may occur on decadal to orbital timescales [e.g., *Lea et al*., 2000; *Stott et al*., 2002; *Mann et al*., 2009; *Emile-Geay et al*., 2013]. It thus stands to reason that zonal shifts in the mean position of deep convection may drive a significant fraction of observed millennial- to orbital-scale variability in Mulu stalagmite δ^{18}O records.

6. Conclusion

Vadose water mixing is the primary karst process that governs the transformation of rainfall-to-dripwater δ^{18}O at Gunung Mulu in northern Borneo. The Mulu karst system acts as a low-pass filter of 3–10+ months, with dripwater δ^{18}O reflecting a smoothed version of amount-weighted local rainfall δ^{18}O. Relatively rapid water transit times allow for large ENSO-related variations in local rainfall δ^{18}O of 6–8‰ to be preserved as dripwater δ^{18}O variations of 2.5–5‰, enabling the reconstruction of past ENSO variability from sufficiently fast-growing Borneo stalagmites. Variations in dripwater residence time, precipitation amount weighting, and ENSO asymmetry likely contribute to systematic offsets between overlapping stalagmite δ^{18}O records documented at our site [*Partin et al*., 2007; *Carolin et al*., 2013]. Longer dripwater δ^{18}O time series, as well as a larger set of monitored drips, are required to assess the role of potential nonlinearities in karst flow patterns through time.

This study demonstrates the power of generating modern rainfall and dripwater isotope time series at sites where paleoclimate reconstructions from stalagmites exist. In addition to highlighting the utility of site-specific monitoring of water isotopes for stalagmite δ^{18}O interpretation, our results demonstrate the importance of replicating stalagmite δ^{18}O records, especially for quantitative reconstructions of ENSO variance.

Acknowledgments

The authors wish to thank the Gunung Mulu National Park staff, Eleanor Middlemas, Danja Mewes, Sang Chen, and Niko Sluzki for their assistance during fieldwork and the Mulu Meteorological Station staff for overseeing the collection of the daily rainfall samples. We also gratefully acknowledge the Mulu Caves Project for providing invaluable information about the Mulu karst system and an anonymous reviewer for comments that greatly improved the manuscript. Permits for this work were granted by the Malaysian Economic Planning Unit, the Sarawak State Planning Unit, and the Sarawak Forestry Department. This work was supported by NSF grant 0645291 to K.M.C., and J.W.M. was funded by a NSF Graduate Research Fellowship. Observational data sets of Mulu rainfall and dripwater isotopes used in this study can be found in the supporting information.

M. Bayani Cardenas thanks one anonymous reviewer for his/her assistance in evaluating this paper.

References

Ayalon, A., M. Bar-Matthews, and E. Sass (1998), Rainfall-recharge relationships within a karstic terrain in the eastern Mediterranean semi-arid region, Israel: Delta O-18 and delta D characteristics, *J. Hydro.*, *207*(1–2), 18–31.

Ayliffe, L. K., et al. (2013), Rapid interhemispheric climate links via the Australasian monsoon during the last deglaciation, *Nat. Commun.*, *4*, 2908.

Baker, A., C. Bradley, S. J. Phipps, M. Fischer, I. J. Fairchild, L. Fuller, C. Spötl, and C. Azcurra (2012), Millennial-length forward models and pseudoproxies of stalagmite δ^{18}O an example from NW Scotland, *Clim. Past.*, *8*(4), 1153–1167.

Baker, A., C. Bradley, and S. J. Phipps (2013), Hydrological modeling of stalagmite δ^{18}O response to glacial-interglacial transitions, *Geophys. Res. Lett.*, *40*, 3207–3212, doi:10.1002/grl.50555.

Berkelhammer, M., A. Sinha, M. Mudelsee, H. Cheng, R. L. Edwards, and K. Cannariato (2010), Persistent multidecadal power of the Indian Summer Monsoon, *Earth Planet. Sci. Lett.*, *290*(1–2), 166–172.

Bradley, C., A. Baker, C. N. Jex, and M. J. Leng (2010), Hydrological uncertainties in the modelling of cave drip-water δ^{18}O and the implications for stalagmite palaeoclimate reconstructions, *Quat. Sci. Rev.*, *29*(17–18), 2201–2214.

Carolin, S. A., K. M. Cobb, J. F. Adkins, B. Clark, J. L. Conroy, S. Lejau, J. Malang, and A. A. Tuen (2013), Varied response of western Pacific hydrology to climate forcings over the last glacial period, *Science*, *340*(6140), 1564–1566.

Cheng, H., R. L. Edwards, W. S. Broecker, G. H. Denton, X. Kong, Y. Wang, R. Zhang, and X. Wang (2009), Ice age terminations, *Science*, *326*(5950), 248–252.

Cobb, K. M., J. F. Adkins, J. W. Partin, and B. Clark (2007), Regional-scale climate influences on temporal variations of rainwater and cave dripwater oxygen isotopes in northern Borneo, *Earth Planet. Sci. Lett.*, *263*(3–4), 207–220.

Cruz, F. W., S. J. Burns, I. Karmann, W. D. Sharp, M. Vuille, A. O. Cardoso, J. A. Ferrari, P. L. S. Dias, and O. Viana (2005a), Insolation-driven changes in atmospheric circulation over the past 116,000 years in subtropical Brazil, *Nature*, *434*(7029), 63–66.

Cruz, F. W., I. Karmann, O. Viana, S. J. Burns, J. A. Ferrari, M. Vuille, A. N. Sial, and M. Z. Moreira (2005b), Stable isotope study of cave percolation waters in subtropical Brazil: Implications for paleoclimate inferences from speleothems, *Chem. Geol.*, *220*(3–4), 245–262.

Dansgaard, W. (1964), Stable isotopes in precipitation, *Tellus*, *16*(4), 436–468.

Dorale, J. A., and Z. H. Liu (2009), Limitations of Hendy test criteria in judging the paleoclimatic suitability of speleothems and the need for replication, *J. Cave Karst Stud.*, *71*(1), 73–80.

Emile-Geay, J., K. M. Cobb, M. E. Mann, and A. T. Wittenberg (2013), Estimating central equatorial Pacific SST variability over the past millennium. Part I: Methodology and validation, *J. Clim.*, *26*(7), 2302–2328.

Fleitmann, D., S. J. Burns, U. Neff, M. Mudelsee, A. Mangini, and A. Matter (2004), Palaeoclimatic interpretation of high-resolution oxygen isotope profiles derived from annually laminated speleothems from Southern Oman, *Quat. Sci. Rev.*, *23*(7–8), 935–945.

Frappier, A., D. Sahagian, L. A. Gonzalez, and S. J. Carpenter (2002), El Niño events recorded by stalagmite carbon isotopes, *Science*, *298*(5593), 565–565.

Frappier, A. B., D. Sahagian, S. J. Carpenter, L. A. González, and B. R. Frappier (2007), Stalagmite stable isotope record of recent tropical cyclone events, *Geology*, *35*(2), 111.

Genty, D., et al. (2014), Rainfall and cave water isotopic relationships in two South-France sites, *Geochim. Cosmochim. Acta*, *131*, 323–343.

Griffiths, M. L., et al. (2009), Increasing Australian–Indonesian monsoon rainfall linked to early Holocene sea-level rise, *Nat. Geosci.*, *2*(9), 636–639.

Jex, C. N., A. Baker, I. J. Fairchild, W. J. Eastwood, M. J. Leng, H. J. Sloane, L. Thomas, and E. Bekaroğlu (2010), Calibration of speleothem δ^{18}O with instrumental climate records from Turkey, *Global Planet. Change*, *71*(3–4), 207–217.

Jex, C. N., S. J. Phipps, A. Baker, and C. Bradley (2013), Reducing uncertainty in the climatic interpretations of speleothem $\delta^{18}O$, *Geophys. Res. Lett.*, *40*, 2259–2264, doi:10.1002/grl.50467.

Kaplan, A., M. A. Cane, Y. Kushnir, A. C. Clement, M. B. Blumenthal, and B. Rajagopalan (1998), Analyses of global sea surface temperature 1856–1991, *J. Geophys. Res.*, *103*, 18,567–18,589, doi:10.1029/97JC0173.

Kleeman, R., and S. B. Power (2000), Modulation of ENSO variability on decadal and longer timescales, in *El Niño and the Southern Oscillation: Multiscale Variability and Global and Regional Impacts*, edited by H. F. Diaz and V. Markgraf, pp. 413–442, Cambridge Univ. Press, Cambridge, U. K.

Kurita, N., K. Ichiyanagi, J. Matsumoto, M. D. Yamanaka, and T. Ohata (2009), The relationship between the isotopic content of precipitation and the precipitation amount in tropical regions, *J. Geochem. Explor.*, *102*(3), 113–122.

Lachniet, M. S. (2004), A 1500-year El Niño/Southern Oscillation and rainfall history for the Isthmus of Panama from speleothem calcite, *J. Geophys. Res.*, *109*, D20117, doi:10.1029/2004JD004694.

Lawrence, J. R., S. D. Gedzelman, D. Dexheimer, H. K. Cho, G. D. Carrie, R. Gasparini, C. R. Anderson, K. P. Bowman, and M. I. Biggerstaff (2004), Stable isotopic composition of water vapor in the tropics, *J. Geophys. Res.*, *109*, D06115, doi:10.1029/2003JD004046.

Lea, D. W., D. K. Pak, and H. J. Spero (2000), Climate impact of late quaternary equatorial Pacific sea surface temperature variations, *Science*, *289*(5485), 1719–1724.

LeGrande, A. N., and G. A. Schmidt (2009), Sources of Holocene variability of oxygen isotopes in paleoclimate archives, *Clim. Past.*, *5*(3), 441–455.

Lewis, S. C., A. N. LeGrande, M. Kelley, and G. A. Schmidt (2010), Water vapour source impacts on oxygen isotope variability in tropical precipitation during Heinrich events, *Clim. Past.*, *6*(3), 325–343.

Mann, M. E., Z. Zhang, S. Rutherford, R. S. Bradley, M. K. Hughes, D. Shindell, C. Ammann, G. Faluvegi, and F. Ni (2009), Global signatures and dynamical origins of the Little Ice Age and Medieval Climate Anomaly, *Science*, *326*(5957), 1256–1260.

McDonald, J. (2004), The 2002–2003 El Niño recorded in Australian cave drip waters: Implications for reconstructing rainfall histories using stalagmites, *Geophys. Res. Lett.*, *31*, L22202, doi:10.1029/2004GL020859.

McPhaden, M. J., and X. B. Zhang (2009), Asymmetry in zonal phase propagation of ENSO sea surface temperature anomalies, *Geophys. Res. Lett.*, *36*, L13703, doi:10.1029/2009GL038774.

Meckler, A. N., M. O. Clarkson, K. M. Cobb, H. Sodemann, and J. F. Adkins (2012), Interglacial hydroclimate in the tropical West Pacific through the late Pleistocene, *Science*, *336*(6086), 1301–1304.

Mickler, P. J., J. L. Banner, L. Stern, Y. Asmerom, R. L. Edwards, and E. Ito (2004), Stable isotope variations in modern tropical speleothems: Evaluating equilibrium vs. kinetic isotope effects, *Geochim. Cosmochim. Acta*, *68*(21), 4381–4393.

Moerman, J. W., K. M. Cobb, J. F. Adkins, H. Sodemann, B. Clark, and A. A. Tuen (2013), Diurnal to interannual rainfall $\delta^{18}O$ variations in northern Borneo driven by regional hydrology, *Earth Planet. Sci. Lett.*, *369–370*, 108–119.

Okumura, Y. M., and C. Deser (2010), Asymmetry in the duration of El Niño and La Niña, *J. Clim.*, *23*(21), 5826–5843.

Oster, J. L., I. P. Montañez, and N. P. Kelley (2012), Response of a modern cave system to large seasonal precipitation variability, *Geochim. Cosmochim. Acta*, *91*, 92–108.

Pape, J. R., J. L. Banner, L. E. Mack, M. Musgrove, and A. Guilfoyle (2010), Controls on oxygen isotope variability in precipitation and cave drip waters, central Texas, USA, *J. Hydro.*, *385*(1–4), 203–215.

Partin, J. W., K. M. Cobb, J. F. Adkins, B. Clark, and D. P. Fernandez (2007), Millennial-scale trends in West Pacific warm pool hydrology since the Last Glacial Maximum, *Nature*, *449*(7161), 452–455.

Partin, J. W., et al. (2012), Relationship between modern rainfall variability, cave dripwater, and stalagmite geochemistry in Guam, USA, *Geochem. Geophys. Geosyst.*, *13*, Q03013, doi:10.1029/2011GC003930.

Partin, J. W., K. M. Cobb, J. F. Adkins, A. A. Tuen, and B. Clark (2013a), Trace metal and carbon isotopic variations in cave dripwater and stalagmite geochemistry from northern Borneo, *Geochem. Geophys. Geosyst.*, *14*, 3567–3585, doi:10.1002/ggge.20215.

Partin, J. W., et al. (2013b), Multidecadal rainfall variability in South Pacific Convergence Zone as revealed by stalagmite geochemistry, *Geology*, *41*(11), 1143–1146.

Reynolds, R. W., N. A. Rayner, T. M. Smith, D. C. Stokes, and W. Q. Wang (2002), An improved in situ and satellite SST analysis for climate, *J. Clim.*, *15*(13), 1609–1625.

Rozanski, K. A.-A., L. Araguás-Araguás, and R. Gonfiantini (1993), Isotopic patterns in modern global precipitation, *Geophys. Monogr. Ser.*, *78*, 1–36.

Schmidt, G. A., A. N. LeGrande, and G. Hoffmann (2007), Water isotope expressions of intrinsic and forced variability in a coupled ocean-atmosphere model, *J. Geophys. Res.*, *112*, D10103, doi:10.1029/2006JD007781.

Sinha, A., K. G. Cannariato, L. D. Stott, H. Cheng, R. L. Edwards, M. G. Yadava, R. Ramesh, and I. B. Singh (2007), A 900-year (600 to 1500 A.D.) record of the Indian summer monsoon precipitation from the core monsoon zone of India, *Geophys. Res. Lett.*, *34*, L16707, doi:10.1029/2007GL030431.

Stott, L., C. Poulsen, S. Lund, and R. Thunell (2002), Super ENSO and global climate oscillations at millennial time scales, *Science*, *297*(5579), 222–226.

Treble, P. C., C. Bradley, A. Wood, A. Baker, C. N. Jex, I. J. Fairchild, M. K. Gagan, J. Cowley, and C. Azcurra (2013), An isotopic and modelling study of flow paths and storage in Quaternary calcarenite, SW Australia: Implications for speleothem paleoclimate records, *Quat. Sci. Rev.*, *64*, 90–103.

Vimeux, F., G. Tremoy, C. Risi, and R. Gallaire (2011), A strong control of the South American SeeSaw on the intra-seasonal variability of the isotopic composition of precipitation in the Bolivian Andes, *Earth Planet. Sci. Lett.*, *307*(1–2), 47–58.

Waltham, A. C., and D. B. Brook (1980), Symposium on the geomorphology of the Mulu Hills.8. Cave development in the Melinau limestone of the Gunung-Mulu National-Park, *Geogr. J.*, *146*, 258–266.

Wang, X., A. S. Auler, R. L. Edwards, H. Cheng, E. Ito, and M. Solheid (2006), Interhemispheric anti-phasing of rainfall during the last glacial period, *Quat. Sci. Rev.*, *25*(23–24), 3391–3403.

Wang, Y. J., H. Cheng, R. L. Edwards, Z. S. An, J. Y. Wu, C. C. Shen, and J. A. Dorale (2001), A high-resolution absolute-dated late Pleistocene monsoon record from Hulu Cave, China, *Science*, *294*(5550), 2345–2348.

Wannier, M. (2009), Carbonate platforms in wedge-top basins: An example from the Gunung Mulu National Park, Northern Sarawak (Malaysia), *Mar. Petrol. Geol.*, *26*(2), 177–207.

Wilford, G. E. (1961), The geology and mineral resources of Brunei and adjacent parts of Sarawak, with description of the Seria and Miri oilfields British Borneo Geol. Surv. Mem., 10.

Zhang, P., et al. (2008), A test of climate, Sun, and culture relationships from an 1810-year Chinese cave record, *Science*, *322*(5903), 940–942.